Performance Optimization of a Large-Scale Ammonia Heat Pump in Off-Design Conditions

Jørgensen, Pernille Hartmund; Ommen, Torben; Markussen, Wiebke Brix; Elmegaard, Brian

Published in:
Proceedings of the 8th Conference on Ammonia and CO₂ Refrigeration Technologies

Link to article, DOI:
10.18462/iir.nh3-co2.2019.0014

Publication date:
2019

Document Version
Peer reviewed version

PAPER ID: XXX[Paper ID]
DOI: 10.18462/iir.[organisers to request DOI from IIR].XXX[DOI Number]

Performance Optimization of a Large-Scale Ammonia Heat Pump in Off-Design Conditions

Pernille Hartmund JØRGENSEN[(a)*], Torben OMMEN[(a)], Wiebke Brix MARKUSSEN [(a)], Brian ELMEGAARD [(a)]

[(a)] Technical University of Denmark
Kgs. Lyngby, 2100, Denmark, *phaj@mek.dtu.dk

ABSTRACT

A thermodynamic model of a 5 MW test and demonstration heat pump, implemented in the district heating network of Copenhagen, is presented. A genetic algorithm was applied to the model for 27 different operating conditions, optimizing the system Coefficient of Performance (COP) by adjusting the available set points (SP) in the heat pump system. Analyzing the optimization result, new SP values depending on the operating conditions were proposed. The potential improvement in COP was between 0.4 % and 2.9 %. A performance map for all operating conditions was presented and discussed. In general the COP increased with decreasing forward temperatures, increasing source temperatures and further an optimum at 80 % heating load was observed within the investigated span of operating conditions.

Keywords: Large-scale heat pump, District heating, COP, Off-design, Optimization.

1. INTRODUCTION

With the aim of transforming the heating sector to rely on renewable resources, large-scale electrical heat pumps (HP) are expected to play an important role in the Danish district heating (DH) system. This is mainly due to the fact that heat pumps 1) can utilize power produced by the increasing share of intermittent renewable sources, 2) recover heat from low temperature heat sources and 3) provide flexibility in an integrated energy system.
From this perspective utility and heat distribution companies (CTR, VEKS, HOFOR) in the Greater Copenhagen Area have built a HP test facility of 5 MW heating capacity, which utilizes ammonia as working fluid, and either sea water or sewage water as heat source. The purpose of this test and demonstration project is to accelerate the use of large-scale heat pumps in the district heating network, through industrial cooperation, research and experimental development (SVAF I, final report). One of the major aims of the project is to demonstrate how a high Coefficient of Performance (COP) can be obtained for varying operating conditions. One approach to fulfilling this goal is to develop a control strategy for continually adjusting the set point (SP) values in the control system to achieve a high COP for different operating conditions.
In the literature, many studies investigate how the COP of a heat pump system varies with part load (PL) conditions and with the chosen control strategy. An observation regarding PL operation reported by both Granryd (1998), Bettanini et al. (2003), Corberán (2016), described how COP increased when the load of the heat pump decreased. The trend was explained by an improved pinch temperature difference in the heat exchangers because of smaller mass flows and thermal fluxes.
Another well described variation in the system COP, relates to the power consumption of auxiliary pumps. This was investigated experimentally in Corberán et al. (2008) where a clear trend between increasing mass flow rates in the secondary loops and increasing system COP was shown.
This paper presents a thermodynamic model of the heat pump installation, and investigates the potential for optimizing the system COP at 27 different operating conditions, by adjusting the value of 14 chosen SPs in the HP system. In order to investigate how the assigned values of these SPs influenced the system COP under different operating conditions, an optimization algorithm was applied. From the optimization result of each SP, it was suggested how the value depended on the operating conditions. The system COP of the HP installation, calculated with the SP values suggested, is presented and discussed.

1.1. HP installation and investigated operating conditions

The HP installation consists of two two-stage heat pumps. In Fig. 1 the heat pump configuration and the heat exchanger network with the heat sink are shown to the left and right, respectively. For each HP the heat is transferred to the DH network in two desuperheaters (DSH), a condenser (CON), a subcooler (SC) and an oil cooler (OC) for each compressor, counting 12 HEXs in total. In design conditions the forward temperature ($T_{\mathrm{DH,forward}}$) is 80 °C, and the return temperature ($T_{\mathrm{DH,return}}$) is 50 °C. The evaporators are connected in parallel with a sea water inlet temperature ($T_{\mathrm{SR,in}}$) of 4 °C and outlet temperature ($T_{\mathrm{SR,out}}$) of 0.5 °C. The heating capacity of 5116 kW is considered as full load capacity (100 %). The 27 different operating conditions considered in this paper is a combination of an inlet source temperature of 4 °C, 11 °C and 18 °C, a forward temperature of 80 °C, 75 °C and 70 °C and finally 100 %, 80 % and 60 % load in heating capacity.

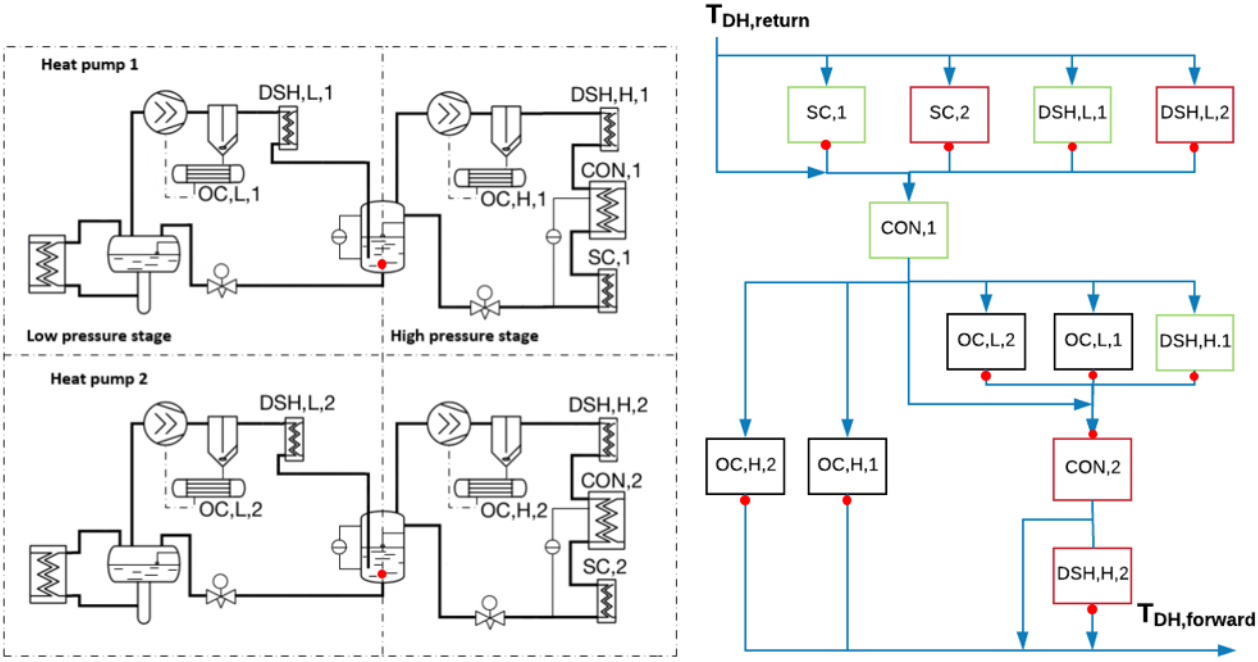

Figure 1: Principle sketch of the heat pump configuration (left) and the sink HEX network (right).

1.2. Available set points in the HP installation

In total 14 SPs were included in the optimization. A red dot in Fig. 1 indicates where in the system the considered SPs refer to. As shown to the right of Fig. 1 the heat exchanger network with the heat sink holds a rather complex design with individual controlled flows going through the different HEXs. This makes the temperature out of the different HEXs (except the condensers) SPs. Changing the flow out of a heat exchanger will change the capacity of the heat exchanger, as well as the pinch temperature difference and entropy generation. The temperature of the DH water going out of a given HEX is referred to by the subscript "DH" followed by the name of the HEX. In total 10 individual SPs related to a temperature out of a HEX in the heat sink were considered.

The saturation temperatures at the intermediate pressures ($T_{\mathrm{M},1}$ and $T_{\mathrm{M},2}$) and a load distribution factor (DF) were considered as individual SPs. The DF was correlated with the inlet temperature of the DH water into CON,2 and they were all related to the load and speed of each compressor.

The last SP included was the temperature glide of the heat source ($\Delta T_{\mathrm{SR}} = T_{\mathrm{SR,in}} - T_{\mathrm{SR,out}}$) (not shown in Fig. 1). This SP depended on the frequency of the installed pumps. The upper limit of the glide is restricted to the risk of ice formation in the evaporators, and it is for this study determined by an outlet temperature of 0 °C for water with a salinity of 2%.

For each set point, a default value based on operation at design conditions, are given from the heat pump supplier. These default values are not disclosed in this paper, for the sake of the heat pump supplier's interest, but are known to the authors by insight in the quotation material. The COP obtained with the thermodynamic model and the default SP values used in all 27 different operating conditions are referred to as $\mathrm{COP_{default}}$.

2. METHODS

The HP installation has been modelled with respect to the specific components installed, and the system layout proposed by the HP supplier. The compressors used were screw compressors and the heat exchangers were mainly plate heat exchangers. Information about the individual characteristics of components were supplied by the respective suppliers. This included the efficiencies related to the compressors, the heat transfer area and heat transfer coefficients of the heat exchangers.
The model of the HP installation was implemented in the Engineering Equation solver, F-Chart (1992) and further combined with a genetic algorithm for optimization from MATLAB, MathWorks (1984).

2.1. Capacity and load distribution

The total capacity of the HP was the sum of every HEX connected to the heat sink, expressed by Eq. (1).

$$\dot{Q}_{\text{total}} = \sum_{k} \sum_{n} \dot{Q}_{DSH,k,n} + \dot{Q}_{\text{CON},n} + \dot{Q}_{\text{SC},n} + \dot{Q}_{\text{OC},k,n}\,, \tag{1}$$

where the index *n* indicated whether the HEX belongs to HP cycle 1 or 2, and *k* to the pressure level.
The distribution of load between the HPs was given by the temperature of the DH water into the condenser of HP 2 ($T_{\text{DH,con,2,in}}$). This temperature was calculated by Eq. (2).

$$T_{\text{DH,con,2,in}} = \frac{(T_{\text{DH,forward}} - T_{\text{DH,return}})}{100} \cdot \text{DF} + T_{\text{DH,return}}\,, \tag{2}$$

where DF was the load distribution factor given as a SP in the control system of the HP.

2.2. Heat exchangers and UA-values

Based on the technical specification of the chosen HEXs, a UA-value was determined for each HEX. For each HEX an energy balance was applied for the hot side (Eq. (3)) and the cold side (Eq. (4)), together with and equation for the overall heat transfer (Eq. (5)).

$$\dot{Q}_{\text{HEX}} = \dot{m}_{\text{ref},k,n} \cdot (h_{\text{out}} - h_{\text{in}}), \tag{3}$$

$$\dot{Q}_{\text{HEX}} = \dot{m}_{\text{DH,HEX}} \cdot (h_{\text{DH,out}} - h_{\text{DH,in}}), \tag{4}$$

$$\dot{Q}_{\text{HEX}} = \text{UA} \cdot \text{MTD}_{\text{approx}}, \tag{5}$$

where $\text{MTD}_{\text{approx}}$ was calculated by the CM2 approximation suggested in Chen (1987).
Special attention was given to the split between desuperheating and the condensation in each HP cycle. For the actual operating conditions the saturation point could either occur in the desuperheater or in the condenser. This was accounted for with a moving boundary model allowing superheated ammonia in the condenser or two phase ammonia in the desuperheater.
To account for a change in the overall heat transfer coefficient with a different mass flow rate on both sides in the HEX, Eq. (6) and (7) based on Pierobon et al. (2014) were used.

$$\frac{UA}{(UA)_{\text{des}}} = \frac{f_{\text{DH}}\ f_{\text{ref}}\,(h_{\text{DH,des}} + h_{\text{ref,des}}\,)}{f_{\text{DH}}\,h_{\text{DH,des}} + f_{\text{ref}}\,h_{\text{ref,des}}}\,, \tag{6}$$

$$f = \frac{h}{h_{\text{des}}} = \left(\frac{\dot{m}}{\dot{m}_{\text{des}}}\right)^{\gamma}, \tag{7}$$

where $h_{\text{DH,des}}$ and $h_{\text{ref,des}}$ were the mean convective resistance at design conditions for both sides of a given HEX, $\dot{m}_{\text{des}}$ was the mass flow rate through the heat exchanger at design conditions and $\dot{m}$ the mass flow rate in off design. The exponent γ was 0.784, 0.445 and 0.351 for single phase fluids, condensation and evaporation, respectively, taken from the heat transfer correlations of Martin (1996), Longo et al. (2015) and Amalfi et al. (2016).

2.3. Compressor efficiency and oil cooling

The isentropic efficiency, volumetric efficiency and performance reduction in part load were calculated based on a given cooling capacity and compressor power for many different operating conditions obtained in the

technical specifications provided by the manufacturer. Furthermore, also the oil flows for the compressors in different operation conditions were obtained in the specifications.
The compressor power was calculated by Eq. (8).

$$\dot{W}_{\mathrm{comp,k,n}} = \dot{m}_{\mathrm{ref},k,n} \cdot (h_{2\mathrm{w}} - h_1), \quad (8)$$

where the subscript 1 and 2 refers to the inlet and outlet condition, respectively, and h_{2w} was obtained by Eq.(9)

$$\eta_{\mathrm{is}} = \frac{h_{2,\mathrm{s}} - h_1}{h_{2,w} - h_1} \quad (9)$$

The oil supplied to the compressor exchanged heat with the gas. This was modelled by Eq. (10), (11) and (12) as an internal heat exchange between the ammonia and the oil, after the compression process, with a common discharge temperature of the two fluids.

$$\dot{Q}_{\mathrm{oil}} = \dot{m}_{\mathrm{ref},k,n} \cdot (h_2 - h_{2\mathrm{w}}) \quad (10)$$

$$\dot{Q}_{\mathrm{oil}} = \dot{m}_{\mathrm{oil}} \cdot c_{p,\mathrm{oil}} \cdot \left(T_{\mathrm{oil,out}} - T_{\mathrm{oil,in}}\right) \quad (11)$$

$$T_{\mathrm{oil,out}} = T_2 \quad (12)$$

The heat exchanged between the refrigerant and the oil was equal to the capacity of the given oil cooler connected to the heat sink.
The rotational speed of the compressors was calculated by Eq. (13).

$$N = \frac{60 \cdot \dot{m}_{\mathrm{ref}} \cdot v_{\mathrm{in}}}{\eta_{\mathrm{vol}} \cdot V_{\mathrm{COMP}}}, \quad (13)$$

where $v_{\mathrm{in}}$was the specific volume at the inlet of the compressor, V_{COMP} the amount of gas compressed in one rotation and η_{vol}, the volumetric efficiency.

2.4. Auxiliary power and system COP

The power used for pumping the source and sink through the related heat exchangers, pipes, filters etc. was calculated by eq. 14

$$\dot{W}_{\mathrm{pump}} = k \cdot \dot{V}^3, \quad (14)$$

where *k* was a constant including density of the fluid, cross-sectional area and friction factors. $\dot{V}$ was the volumetric flow rate of the fluid.
The system COP was then defined as Eq. 15

$$\mathrm{COP}_{\mathrm{sys}} = \frac{\dot{Q}_{\mathrm{total}}}{\dot{W}_{\mathrm{pump,DH}} + \dot{W}_{\mathrm{pump,SR}} + \sum_k \sum_n \dot{W}_{\mathrm{COMP},k,n}} \quad (15)$$

2.5. Model constraints

In order to ensure that the simulations results were physically feasible, a number of constraints were implemented in model. These included a minimum pinch temperature difference of 0.5 K in all HEXs, a minimum mass flow rate in bypass flows of 0.1 kg/s and a maximum rotational speed of 3600 for the compressors. If a simulation result violated any of these constraints, a Boolean parameter, was assigned to "*error*". This was used, as described below, in the optimization algorithm to ensure the technical feasibility of the solution.

2.6. Optimisation algorithm

In order to investigate if the system COP could be optimized by any of the 14 considered SP values the thermodynamic model was combined with a genetic algorithm. The algorithm was given "$-\mathrm{COP} + \sum error$" as objective function to minimize, with a population size of 60, and a stop criteria when the variation in the objective function was equal to or less than 10^{-5}. The EES model consisted of 840 equations, and running the optimization algorithm for one operating condition took ~12 hours.
The optimization algorithm was applied in two iterations, in order to reduce the number of SPs. This is further explained in Sec. 3.1. The SPs found by applying the optimization algorithm, were further analyzed in order to deduce a dependency on the operating conditions. This resulted in a suggested value for each SP in all operating conditions.

2.7. Performance mapping

The value suggested for each SP at a given operating condition was implemented in the thermodynamic model, and a COP was calculated for the 27 different operating conditions. These COPs are further referred to as COP_{opt}. Furthermore, the percentage differences between COP_{opt} and $COP_{default}$ were calculated for each operating condition.

3. RESULTS

The results presented are divided into two subsections. Section 3.1 presents the dependencies between each SP and the operating conditions as well as a suggested SP value. Section 3.2 presents COP_{opt} for the different operating conditions, together with the potential improvement in COP.

3.1. Set point value and dependency

In the first iteration of optimization, all 14 SPs were included in the algorithm. This preliminary result revealed that the temperatures, $T_{DH,DSH,H,1}$ and $T_{DH,DSH,H,2}$, should be kept "low" in order to ensure a high capacity of the current desuperheater. Contrary, the temperatures $T_{DH,OC,H,1}$ and $T_{DH,OC,H,2}$ should be kept high, as this increased the mass flow rate of DH through CON,2 and reduced the condensation temperature. Furthermore it was seen that the total capacity of the first four parallel HEXs (SC1, SC2, DSH,L,1 + DSH,L,2) should be as high as possible. To ensure this the by-pass flow was in the second iteration given as an input of 0.5 kg/s and $T_{DH,SC,2}$ as a free variable.

The trends described above resulted in the SP dependencies for $T_{DH,DSH,H,1}$, $T_{DH,DSH,H,2}$, $T_{DH,OC,H,1}$ and $T_{DH,OC,H,2}$ listed in table 1. With these implemented the dependency shown in Table 1 on the source inlet temperature, the forward temperature and load was deduced from the second iteration of optimization, for the SPs: $T_{DH,SC,1}$, $T_{DH,SC,2}$, $T_{DH,OC,L,1}$, $T_{DH,OC,L,2}$, $T_{M.1}$, $T_{M.2}$, ΔT_{SR} and the distribution factor, DF.

Table 1: Set point values deduced from the optimization results.

SP variable	**Dependency**									
	Internal									
$T_{DH,DSH,H,1}$ [°C]		$T_{DH,CON,1out} + 5$								
$T_{DH,DSH,H,2}$ [°C]		$T_{DH,CON,2out} + 5$								
	Constant									
$T_{DH,OC,H,1}$ [°C]		90								
$T_{DH,OC,H,2}$ [°C]		95								
	$T_{DH,forward}$:	**80 °C**			**75 °C**			**70 °C**		
$T_{DH,SC,1}$ [°C]		53.4			52.6			51.8		
$T_{DH,SC,2}$ [°C]		53.9			52.9			51.8		
	$T_{SR,in}$	**4 °C**			**11 °C**			**18 °C**		
$T_{DH,OC,L,1}$, $T_{DH,OC,L,2}$ [°C]		71.1			69.9			68.5		
	$T_{SR,in}$	**4 °C**			**11 °C**			**18 °C**		
	$T_{DH,forward}$	**80 °C**	**75 °C**	**70 °C**	**80 °C**	**75 °C**	**70 °C**	**80 °C**	**75 °C**	**70 °C**
$T_{M,1}$, $T_{M,2}$ [°C]		32.5	30.3	29.2	33.0	31.6	31.0	34.5	34.3	33.7
	$T_{SR,in}$	**4 °C**			**11 °C**			**18 °C**		
	Load	**100 %**	**80 %**	**60 %**	**100 %**	**80 %**	**60 %**	**100 %**	**80 %**	**60 %**
ΔT_{SR} [K]		4.0	3.7	3.2	4.2	3.8	3.2	4.6	4.3	3.8
DF [-]		56.2	54.6	53.7	55.5	54.0	53.4	56.2	54.4	54.1

Fig. 2 shows the optimization results for the temperature glide of the source, ΔT_{SR}. Here it was chosen to take an average value of the glide for each forward temperature at a given source temperature and heating load. The average values are shown in black in Fig. 2, and the values are presented in Table 1.

The temperature out of the subcoolers as well as the temperature out of the oil coolers could in a similar way be reduced to a single dependency, while the distribution factor and the intermediate temperature also depended on two of the three conditions. This is reflected in Table 1.

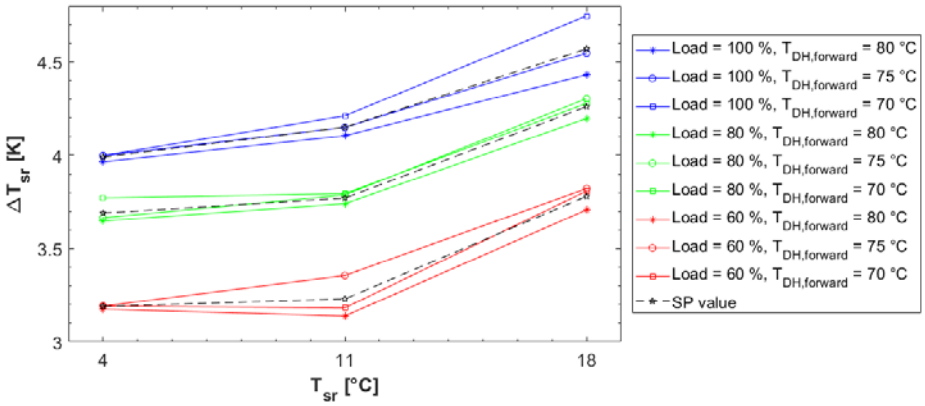

Figure 2: Optimization result of the source glide for 27 different operating conditions. The symbols in black indicate the average value suggested in Table 1

Regarding the temperatures out of the desuperheaters at the low stages, the second iteration showed a trend of the two temperatures being equal to each other. The exact SP values for $T_{DH,DSH,L,1}$ and $T_{DH,DSH,L2}$, presented in Table 2, were obtained by implementing this relation ($T_{DH,DSH,L,1} = T_{DH,DSH,L,2}$) together with the values for the rest of the SPs (Table 1), in the thermodynamic model.
As seen in Table 2 the SP values depended on all three variables in the operating conditions.

Table 2: Set point values of $T_{DH,DSH,L,1}$, $T_{DH,DSH,L,2}$ [°C]

4 °C								
100 %			**80 %**			**60 %**		
80 °C	**75 °C**	**70 °C**	**80 °C**	**75 °C**	**70 °C**	**80 °C**	**75 °C**	**70 °C**
55.0	54.1	53.4	54.7	53.7	52.8	54.2	53.3	52.3
11 C								
100 %			**80 %**			**60 %**		
80 °C	**75 °C**	**70 °C**	**80 °C**	**75 °C**	**70 °C**	**80 °C**	**75 °C**	**70 °C**
54.2	53.4	52.9	54.0	53.2	52.6	53.6	52.9	52.3
18 °C								
100 %			**80 %**			**60 %**		
80 °C	**75 °C**	**70 °C**	**80 °C**	**75 °C**	**70 °C**	**80 °C**	**75 °C**	**70 °C**
53.8	53.4	52.6	53.6	53.2	52.4	53.4	52.9	52.2

3.2. Performance map and potential improvement in COP

Fig. 3a shows the COP_{opt} as calculated in the 27 operating conditions, with the SPs suggested in Table 1 and 2. In Fig. 3a it is shown that the COP increased with both an increasing source temperature (different line colors) and decreasing forward temperatures (different symbols). Both can be explained by the lower temperature lifts and compression pressure ratios.
As also shown on Figure 3a, the COP is highest at 80 % load in all cases. The reason for this was seen by smaller pinch temperatures in the HEXs both for the evaporators and the HEXs connected to the heat sink. Furthermore, the optimal temperature glide decreased with part load, which also contributed to a higher evaporation temperature. At a load of 60 % the system COP decreased again. This was due to decreasing isentropic efficiencies in part load. The highest COP of 4.3 was found at a forward temperature of 70 °C, a source inlet temperature of 18 °C and 80 % load, while the lowest COP of 3.4 was found at a forward temperature of 80 °C, a source inlet temperature of 4 °C and 60 % load.

Fig. 3b shows the percentage difference, between the COP_{opt} and the $COP_{default}$, and can be seen as the potential improvement in COP by applying the suggested SP values. The difference varies between 0.4 % and 2.9 %, with the highest improvement found for a source temperature of 4 °C, forward temperature of 70 °C and 60 % heating load. In general, the potential improvement increases for lower forward temperatures.

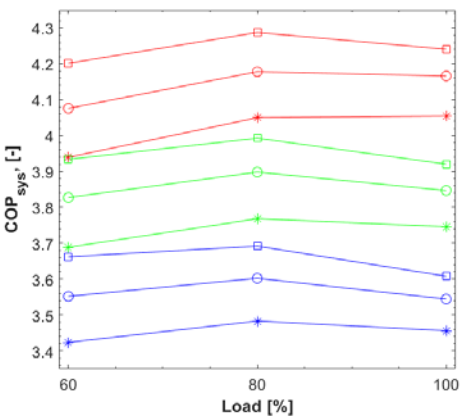

Figure 3a

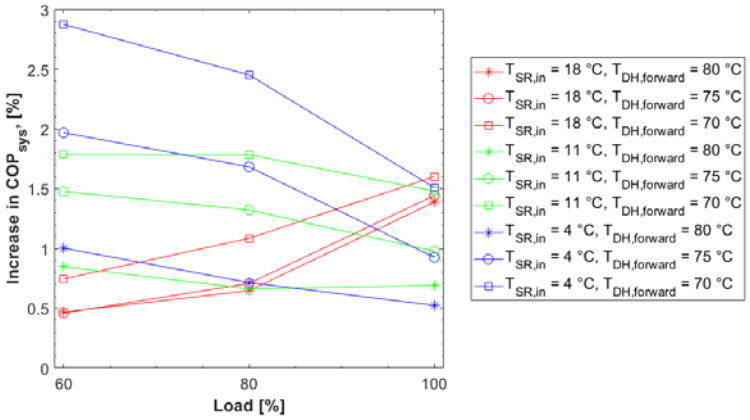

Figure 3b

Figure 3a: System COP_{opt} for all 27 operating conditions based on the suggested SP values.
Figure 3b: Potential improvement in system COP compared to $COP_{default}$. The legend applies to both figures.

Comparing the COP_{opt} presented in Fig. 3a, with the COP obtained by the optimization in the second iteration, showed a reduction of up to 0.3% in the potential improvement of COP. For 9 out of the 27 cases a negligible difference in the potential improvement was found.

4. DISCUSSION

The potential improvement of performance found by applying the optimization algorithm to the HP model can in general be considered as rather low. Therefore it must be expected that the improvement will be difficult to measure and achieve in practice.

The optimization result suggested a high mass flow rate through the HEXs DSH,L,1 + 2, SC,1 + 2 and DSH,H,1 + 2. This will increase the capacity of the HEX and maintain a high UA value. However, a higher mass flow rate will also increase the pressure drop through the HEX, and increase the needed pump power. This drawback for the individual HEXs was not included in the model, but could have an impact on the obtained SP values. In order to validate the current result, as well as extending the understanding of accurate HP modelling, the thermodynamic model will be validated with data for the different operating conditions, once the plant is in operation. From the data it is expected to achieve empirical correlations for the variations in heat transfer and pressure drop in the heat exchangers. This will give further understanding of how the pinch temperatures in the HEXs are affected, and how the pressure losses in the heat sink and source affect the associates pump power.

In order to have a more detailed picture of the COP in the present operation span, it is considered as further work to include more operation points. This will also give the opportunity to develop correlations for each set point, as for now only linear interpolation would be applicable.

5. CONCLUSIONS

A genetic algorithm was applied to the thermodynamic heat pump model optimizing for system COP by adjusting the available set points in the heat pump system. Analyzing the SP values obtained by optimization, new SP values depending on the operating conditions were presented. The system COP_{opt} obtained with the suggested SP values, were compared to the system $COP_{default}$ obtained with default SP values as given in design conditions. The potential improvement in COP by the suggested SPs was between 0.4 % and 2.9 %. A performance map for all operating conditions was presented and discussed. The highest system COP of 4.2 was achieved at a forward temperature of 70 °C, a source inlet temperature of 18 °C and 80 % heating capacity. In general the COP increased with decreasing forward temperatures, increasing source temperatures and further an optimum at 80 % heating load was observed within the investigated span of operating conditions.

ACKNOWLEDGEMENTS

This research project was funded by EUDP (Energy Technology Development and Demonstration). "Experimental development of electric heat pumps in the Greater Copenhagen DH system – Phase 2", project number: 64015 – 0571.

NOMENCLATURE

Symbols		*greek*			
A	areal (m^2)	η	efficiency (-)	MTD	mean temp. difference
cp	specific heating capacity (kW/kg*K)	ν	specific volume (m^3/kg)	SP	set point
h	enthalpy (kJ/kg)	ΔT	temperature difference (K)	SR	source
$\dot{m}$	mass flow rate (kg/s)			SC	subcooler
N	Rotational speed (rpm)	*Abbreviations*		OC	oil cooler
p	pressure (bar)	COMP	compressor	*Super- & subscripts*	
$\dot{Q}$	capacity (kW)	CON	condenser	H	high
T	temperature (°C)	COP	coefficient of performance	L	low
U	overall heat transfer coefficient	DF	distribution factor	vol	volumetric
V	volume (m^3)	DH	district heating	is	isentropic
$\dot{V}$	volumetric flow rate (m^3/s)	DSH	desuperheater	ref	refrigerant
$\dot{W}$	work (kW)	HEX	heat exchanger	opt	optimized

REFERENCES

SVAF I, Final Report of "Experimental development of electric heat pumps in the Greater Copenhagen DHsystem, Phase1" https://www.energiforskning.dk/sites/energiteknologi.dk/files/slutrapporter/svaf_i_final_report_2016-02-02.pdf (accessed 19.12.2018)

Granryd E., 1998. Power for fans and pumps in heat exchangers of refrigerating plants, The 1998 International Refrigeration Conference", Purdue University, Lafayette, Indiana, USA.

Bettanini E., Gastaldello, A., Schibuola L., 2003. Simplifies models to simulate part load performance of air conditioning equipments, Eighth International IBPSA Conference, Eindhoven, Netherlands.

Corberán J. M, 2016. New trends and developments in ground –source heat pumps. In: Rees, S. J., Advances in Ground-source Heat Pump Systems, Woodhead Publishing, 359-385.

Corberán, J.M., Radulescu, C., Macia, J. G., 2008. Performance characterisation of a reversible water to water heat pump, 9th IEA Heat Pump Conference, Zurich.

F-chart, Klein, S. A., 1992. Engineering Equation Solver, http://www.fchart.com/ees/ (accessed 19.12.2018).

MathWorks, 1984. MATLAB genetic algorithm. https://se.mathworks.com/help/gads/ga.html (accessed 19.12.2018)

Chen, J. J. J., 1987. Comments on improvements on a replacement for the logarithmic mean. Chemical Engineering Science, Vol 42, No. 10, 2488-2489.

Pierobon, L., Benato, A., Scolari, E., Haglind, F., Stoppato, A., Waste heat recovery technologies for offshore platforms. Applied Energy 136 (2014), 228-241.

Martin, H., 1996. A theoretical approach to predict the performance of chevron-type plate heat exchangers. Chemical Engineering and Processing 35 (1996), 301-310.

Longo, G. A., Righetti, G., Zilio, C., 2015. A new computational procedure for refrigerant condensation inside herringbone-type Brazed Plate Heat Exchangers. International Journal of Heat and Mass Transfer 82 (2015), 530-536.

Amalfi, R. L., Vakili-Farahani, F., Thome, J. R., 2016. Flow boiling and frictional pressure gradients in plate heat exchangers. Part 2: Comparison of literature methods to database and new prediction methods. International Journal of Refrigeration 61 (2016), 185-203.